

Automated model for characterization of VCSEL circuit-level parameters using machine learning

*Original*

Automated model for characterization of VCSEL circuit-level parameters using machine learning / Marchisio, Andrea; Khan, Ihtesham; Tunesi, Lorenzo; Masood, Muhammad Umar; Ghillino, Enrico; Curri, Vittorio; Carena, Andrea; Bardella, Paolo. - ELETTRONICO. - (2023), pp. 264-266. (Intervento presentato al convegno European Conference on Integrated Optics tenutosi a Enschede, Paesi Bassi nel 19-21 Aprile 2023).

*Availability:*

This version is available at: 11583/2978489 since: 2023-05-14T17:07:21Z

*Publisher:*

European Conference on Integrated Optics

*Published*

DOI:

*Terms of use:*

This article is made available under terms and conditions as specified in the corresponding bibliographic description in the repository

*Publisher copyright*

(Article begins on next page)

# Automated Model for Characterization of VCSEL Circuit-level Parameters Using Machine Learning

Andrea Marchisio<sup>1</sup>, Ihtesham Khan<sup>1</sup>, Lorenzo Tunesi<sup>1</sup>, Muhammad Umar Masood<sup>1</sup>,  
Enrico Ghillino<sup>2</sup>, Vittorio Curri<sup>1</sup>, Andrea Carena<sup>1</sup>, and Paolo Bardella<sup>1</sup>

<sup>1</sup> Politecnico di Torino, Corso Duca degli Abruzzi, 24, 10129, Torino, Italy

<sup>2</sup> Synopsys, Inc., 400 Executive Blvd Ste 101, Ossining, NY 10562, United States

paolo.bardella@polito.it

**We propose a machine learning-based model to extract physical parameters characterizing stationary-and-dynamic behavior of a VCSEL. The model is trained with circuit-level simulations of light-current and S21 characteristics. Excellent results are achieved as a relative prediction error.**

**Keywords:** machine learning, VCSEL, physical model, parameters extraction

## INTRODUCTION

In the last decades, a significant number of physical models have been proposed in the literature to describe the complex behavior of edge-emitting or vertical-cavity laser diodes, either with a phenomenological or an empirical approach. With an accurate description of advanced physical effects, these tools allow a better understanding of the laser behavior and the optimization of device properties according to designers' needs. As a drawback, the number of involved physical parameters (geometrical properties, material characteristics, electrical and thermal effects) is generally so large that it may be challenging to find a correct set of parameters fitting experimental laser measurements, starting from the fundamental light-current (L-I) characteristics and the small signal modulation responses (S21). The extraction of these physical parameters from experimental curves can be time-consuming, since it often relies on brute-force minimization routines, trial-and-error approaches, or regression analysis. We propose a Machine Learning (ML) approach to the problem, based on Deep Learning (DL), which can extract from experimental measurements the parameters required by a circuit-level model of a Vertical-Cavity Surface-Emitting Laser (VCSEL) [1], implemented in Synopsys OptSim™ [2]. With respect to other works, which focused on edge emitting devices [3] or required two separate simulations to take into account temperature-dependent effects [4], we propose a single DL-based agent that can deal with all the electrical, optical, and thermal effects considered in OptSim™.

## VERTICAL-CAVITY SURFACE-EMITTING LASER MODEL

For the description of the optical and electrical properties of the VCSEL, we rely on the model available in Synopsys OptSim™ [2], which implements and expands the circuit-level model originally proposed in [1]. There, the explicit spatial dependence of the number of carriers  $N(r, t)$  in the transverse plane is eliminated by assuming cylindrical symmetry and by introducing a two-term Bessel series expansion:

$$N(r, t) = N_0(t) - N_1(t)J_0(\sigma_1 r/R)$$

with  $J_0$  and  $J_1$  Bessel functions of the first kind,  $\sigma_1$  first nonzero root of  $J_1$ , and  $R$  effective radius of the active layer. The temporal evolution of the expansion coefficients  $N_0(t)$  and  $N_1(t)$  is given by the following spatially independent rate equations:

$$\frac{dN_0}{dt} = \frac{\eta_i I}{q} - \frac{N_0}{\tau_n} - \frac{G[\gamma_{00}(N_0 - N_{tr}) - \gamma_{01}N_1]}{1 + \epsilon S} S - \frac{I_l}{q}; \quad \frac{dN_1}{dt} = -\frac{N_1}{\tau_n}(1 + h_{diff}) + \frac{G[\phi_{100}(N_0 - N_{tr}) - \phi_{101}N_1]}{1 + \epsilon S} S$$

with  $\eta_i$  injection efficiency,  $\tau_n$  carrier lifetime,  $G$  gain coefficient,  $N_{tr}$  transparency carrier number,  $I_l$  leakage term,  $\epsilon$  gain compression factor,  $h_{diff}$  diffusion coefficient. The four coefficients  $\gamma_{00}$ ,  $\gamma_{01}$ ,  $\phi_{100}$ ,  $\phi_{101}$  quantify the interaction with the fundamental transverse mode profile, assumed to have a Gaussian profile [1].

The temporal evolution of the photon number  $S$  in the cavity and its associated phase  $\phi$  [5] are described by the following rate equations:

$$\frac{dS}{dt} = -\frac{S}{\tau_p} + \frac{\beta_{sp}N_0}{\tau_n} + \frac{G[\gamma_{00}(N_0 - N_{tr}) - \gamma_{01}N_1]}{1 + \epsilon S}; \quad \frac{d\phi}{dt} = \frac{\alpha}{2} \frac{G[\gamma_{00}(N_0 - N_{tr}) - \gamma_{01}N_1]}{1 + \epsilon S}$$

with  $\tau_p$  photon lifetime,  $\beta_{sp}$  spontaneous emission coefficient,  $\alpha$  linewidth enhancement factor. The output power  $P_{out}$  is obtained from  $S$  through a proper multiplication coefficient  $k_f$ .

The device temperature is dynamically calculated as [6]

$$T = T_{amb} + (IV - P_{out})R_{th} - \tau_{th} \frac{dT}{dt}$$

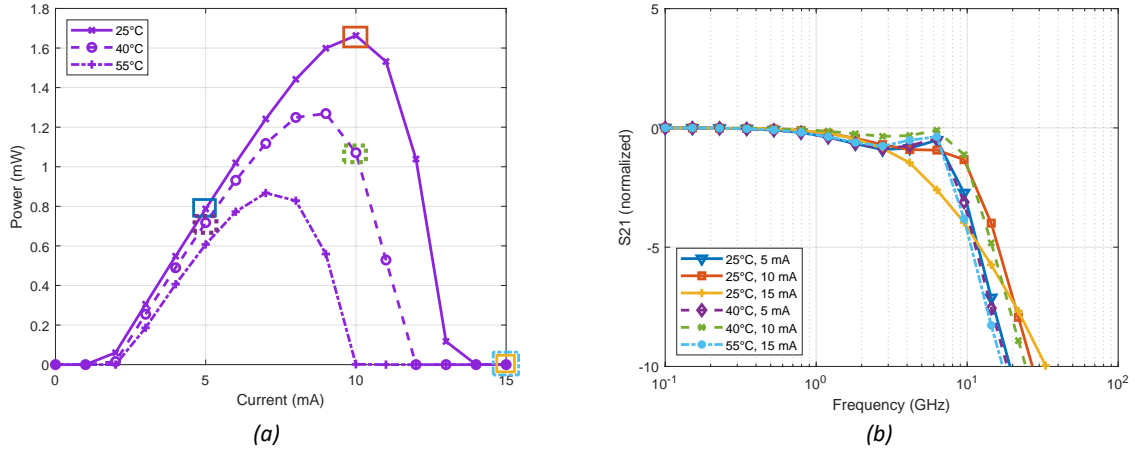


Fig. 1: Example of a VCSEL dataset entry. Markers indicate the samples stored in the recordset. (a) L-I curves at 25 °C, 40 °C, and 55 °C; (b) S21 curves evaluated in the conditions indicated by rectangles in (a).

with  $V$  applied voltage,  $T_{\text{amb}}$  ambient temperature,  $R_{\text{th}}$  thermal impedance and  $\tau_{\text{th}}$  thermal time constant. The parameters  $G$ ,  $N_{\text{t}}$ ,  $I_{\text{l}}$  depend on the device temperature  $T$  through empirical laws:

$$G(T) = G_0 \frac{a_{g0} + a_{g1}T + a_{g2}T^2}{b_{g0} + b_{g1}T + b_{g2}T^2}$$

$$N_{\text{tr}}(T) = N_{\text{tr0}} (c_{n0} + c_{n1}T + c_{n2}T^2)$$

$$I_{\text{l}}(N_0, T) = I_{\text{l0}} \exp \left[ \frac{-a_0 + a_1N_0 + a_2N_0T - a_3/N_0}{T} \right]$$

## DATASET GENERATION & MACHINE LEARNING ENGINE

The dataset is obtained by changing the 22 VCSEL parameters listed in Table 1; for each parameter, a value is randomly generated with uniform distribution in the reported range. During the generation of the random set of values, nonphysical combinations of parameters can be generated, leading, for instance, to thresholds far outside the investigated current ranges. These combinations are discarded and only 14 000 valid records are used in the final data set.

The following values are calculated for each set of random parameters:

- 16 samples from each L-I characteristic, for  $T_{\text{amb}}$  25 °C, 40 °C, and 55 °C, respectively.
- 16 samples of the S21 responses calculated at 5 mA, 10 mA, and 15 mA at 25 °C
- 16 samples of the S21 responses calculated at 5 mA and 10 mA at 40 °C
- 16 samples of the S21 responses calculated at 15 mA at 55 °C

The L-I points are calculated with 16 currents uniformly distributed in the range 0 to 15 mA, while the S21 characteristics are obtained from 16 frequencies logarithmically spaced in the 100 mHz-50 GHz interval. As a result, each record is formed by 192 samples. An example of L-I curves at different temperatures and the corresponding S21 responses are shown in Fig. 1. After the generation of the dataset, the ML-based framework to extract the VCSEL model parameters is finally developed. The proposed ML agent is constructed with a parallel Deep Neural Network (DNN) architecture, meaning that each individual VCSEL parameter is extracted by its own dedicated DNN. Thus, we are able to increase the prediction accuracy by independently optimizing the DNN hyperparameters for each VCSEL parameter under test. In particular, we scanned different combinations of hidden layers number ([2, 3, 4, 5, 6, 7]), of neurons per layer ([20, 30, 50, 100]) and batch size ([100, 200, 500, 1000, 2000]), with fixed learning rate of 0.001. In the proposed DNN model, the Mean Squared Error (MSE) is used as loss function, while *ReLU* is the activation function of each hidden layer. Of the entire dataset, 70% is dedicated to training, while 30% is for testing. The parallel DNN architecture is developed using TensorFlow™ with the Keras API.

## RESULTS AND CONCLUSIONS

The accuracy of the predictions made by a DNN unit is evaluated using the relative prediction error ( $\Delta = \frac{\text{Predicted Value} - \text{Actual Value}}{\text{Actual Value}}$ ) of each considered parameter. The findings of the DL agent are shown in Fig. 2 as a histogram of the relative error of the parameters that are considered, together with the standard deviation ( $\sigma$ ) of the relative prediction error. The most critical parameters are related to the leakage current ( $a_2$  and  $I_{\text{l0}}$ ); for all the considered parameters the error is less than  $\approx 20\%$ . The proposed approach can find a reasonably accurate set of VCSEL parameters in a short time using a fully automated and model-agnostic mechanism. In order to generate the

Table 1: Parameters investigated and corresponding variation ranges for generating dataset.

| Parameters                    | Range                                                              | Parameters                           | Range                                                     |
|-------------------------------|--------------------------------------------------------------------|--------------------------------------|-----------------------------------------------------------|
| Injection efficiency $\eta_i$ | 0.7 to 1                                                           | Transparency carrier $N_{tr}$        | $2 \times 10^6$ to $1 \times 10^7$                        |
| Photons to power $k_f$        | $1 \times 10^{-8}$ W to $6 \times 10^{-8}$ W                       | Gain saturation factor $\varepsilon$ | $1 \times 10^{-6}$ to $5 \times 10^{-6}$                  |
| Carrier lifetime $\tau_n$     | 0.5 ns to 5 ns                                                     | Leakage current factor $I_{l0}$      | 1 A to 2 A                                                |
| Photon lifetime $\tau_p$      | 1.5 ps to 3.5 ps                                                   | Transp. number param. $C_{n0}$       | 1 to 10                                                   |
| Gain coeff. $g_0$             | $1 \times 10^4$ s <sup>-1</sup> to $2 \times 10^5$ s <sup>-1</sup> | Transp. number param. $C_{n1}$       | $-0.1$ K <sup>-1</sup> to $-0.01$ K <sup>-1</sup>         |
| Gain coeff. $a_{g0}$          | $-1 \times 10^4$ to $-4 \times 10^3$                               | Transp. number param. $C_{n2}$       | $0$ K <sup>-2</sup> to $1 \times 10^{-4}$ K <sup>-2</sup> |
| Gain coeff. $a_{g1}$          | $5$ K <sup>-1</sup> to $20$ K <sup>-1</sup>                        | Leakage current param. $a_0$         | 2000 K to 10 000 K                                        |
| Gain coeff. $a_{g2}$          | $0.02$ K <sup>-2</sup> to $0.2$ K <sup>-2</sup>                    | Leakage current param. $a_1$         | $0$ K to $3 \times 10^{-4}$ K                             |
| Gain coeff. $b_{g0}$          | $1 \times 10^3$ to $1 \times 10^4$                                 | Leakage current param. $a_2$         | $1 \times 10^{-9}$ to $4 \times 10^{-8}$                  |
| Gain coeff. $b_{g1}$          | $-100$ K <sup>-1</sup> to $0$ K <sup>-1</sup>                      | Diffusion parameter $h_{diff}$       | 1 to 20                                                   |
| Gain coeff. $b_{g2}$          | $0$ K <sup>-2</sup> to $1$ K <sup>-2</sup>                         | Thermal impedance $R_{th}$           | $500$ K W <sup>-1</sup> to $8000$ K W <sup>-1</sup>       |

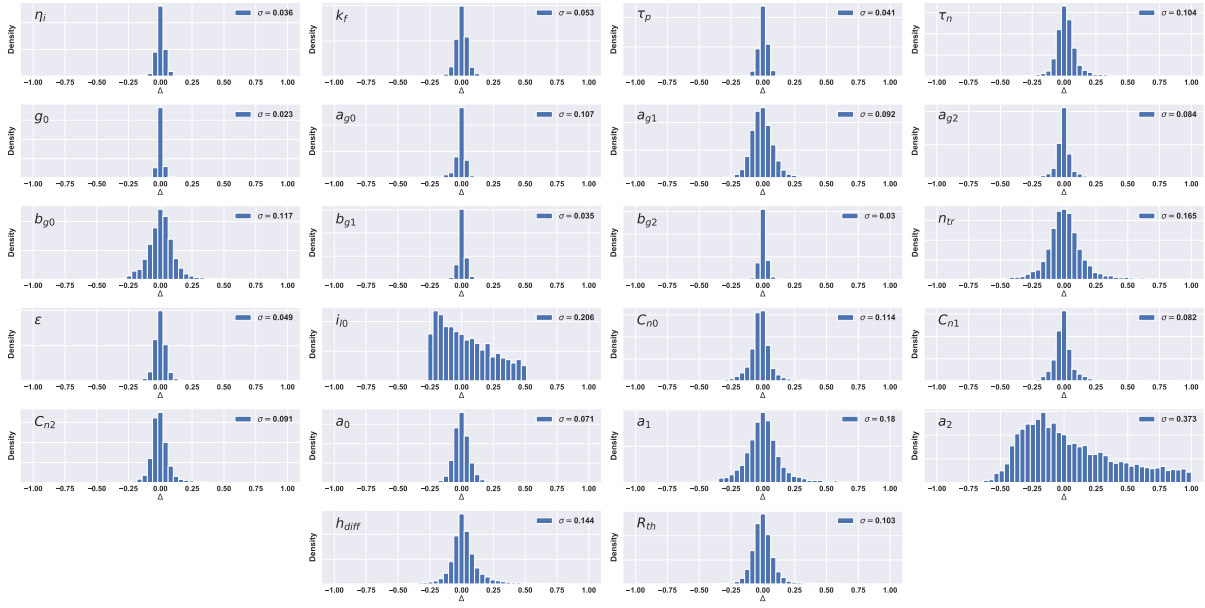


Fig. 2: Relative predicting error of the DL agent for the 22 parameters listed in Table I. In each histogram, the relative error standard deviation is also numerically reported.

dataset and to train the DL agent, the simulation is executed for a few hours on the latest workstations. In addition, the proposed model can easily be scaled up with a high level of accuracy for a larger number of parameters (compared to the 22 parameters that are analyzed in this work) due to its parallel architecture, which has the capability to be rapidly expanded without compromising accuracy. This enables the proposed architecture to be advantageously adapted to study other laser classes.

We present a method that uses DL to extract the essential physical parameters that characterize the stationary and dynamic behavior of the VCSEL source. Circuit-level simulations of the L-I and S21 characteristics of VCSELs, including temperature-related effects, are used to generate the data sets. The proposed technique is fully automated and can be operated for fast and accurate extraction of VCSEL parameters. Furthermore, the suggested scheme is easily scalable to a more vast set of parameters in more complicated models, rather than being restricted to the given set-up.

## References

- [1] P. Mena *et al.*, "A comprehensive circuit-level model of vertical-cavity surface-emitting lasers," *J. Light. Technol.* **17**, 2612–2632 (1999).
- [2] <https://www.synopsys.com/photonic-solutions/pic-design-suite.html>.
- [3] Z. Ma and Y. Li, "Parameter extraction and inverse design of semiconductor lasers based on the deep learning and particle swarm optimization method," *Opt. Express* **28**, 21971–21981 (2020).
- [4] I. Khan *et al.*, "Two-step machine learning assisted extraction of VCSEL parameters," in *2023 SPIE Physics and Simulation of Opto-electronic Devices XXXI*, (SPIE, 2023), pp. 12415–49.
- [5] M. X. Jungo *et al.*, "VISTAS: a comprehensive system-oriented spatiotemporal VCSEL model," *IEEE J. Sel. Top. Quantum Electron.* **9**, 939–948 (2003).
- [6] N. Bewtra *et al.*, "Modeling of quantum-well lasers with electro-opto-thermal interaction," *IEEE J. Sel. Top. Quantum Electron.* **1**, 331–340 (1995).